

Creep and Flow Regimes of Magnetic Domain-Wall Motion in Ultrathin Pt/Co/Pt Films with Perpendicular Anisotropy

P. J. Metaxas,^{1,2,*} J. P. Jamet,¹ A. Mougin,¹ M. Cormier,¹ J. Ferré,¹ V. Baltz,³ B. Rodmacq,³ B. Dieny,³ and R. L. Stamps²

¹Laboratoire de Physique des Solides, Université Paris-Sud, CNRS, UMR 8502, F-91405 Orsay Cedex, France

²School of Physics, M013, University of Western Australia, 35 Stirling Hwy, Crawley WA 6009, Australia

³SPINTEC, URA CNRS/CEA 2512, CEA-Grenoble, 38054 Grenoble Cedex 9, France

(Received 26 February 2007; published 21 November 2007)

We report on magnetic domain-wall velocity measurements in ultrathin Pt/Co(0.5–0.8 nm)/Pt films with perpendicular anisotropy over a large range of applied magnetic fields. The complete velocity-field characteristics are obtained, enabling an examination of the transition between thermally activated creep and viscous flow: motion regimes predicted from general theories for driven elastic interfaces in weakly disordered media. The dissipation limited flow regime is found to be consistent with precessional domain-wall motion, analysis of which yields values for the damping parameter, α .

DOI: 10.1103/PhysRevLett.99.217208

PACS numbers: 75.60.Ch, 62.20.Hg, 75.60.Jk, 75.70.Ak

Understanding the dynamics of an elastic interface driven by a force through a weakly disordered medium is a challenging problem relevant to many physical systems. Examples include domain walls in ferromagnetic [1–3] and ferroelectric [4] materials, vortices in type-II superconductors [5], charge density waves [6], and contact lines during wetting of solids by liquids [7]. While theory predicts three main regimes of motion [5,8–10], only the low force regime of creep has been experimentally studied through direct observation of the interface [1,2,4]. Regimes beyond that of creep, namely, depinning and flow, have, however, been evidenced indirectly via ac susceptibility measurements [11,12]. In this Letter we report on direct observation of magnetic domain-wall motion in ultrathin Pt/Co/Pt films over all motion regimes. This allows for a careful study of the wall velocity, in particular, at the transition from creep to flow and in the high field flow regime, where we consider the internal wall dynamics [13–15].

At zero temperature, an elastic interface in the presence of weak disorder will be pinned for all driving forces, f , below the depinning force, f_{dep} , at which a critical depinning transition [8] occurs [Fig. 1(a)]. At finite temperature the depinning transition becomes smeared due to thermal activation [10] and a finite velocity is then expected for all nonzero forces. This is true even for $f \ll f_{\text{dep}}$, where the thermally activated interface motion is known as creep [5,8]. At the other extreme, once f is sufficiently beyond f_{dep} , disorder becomes irrelevant resulting in a dissipative viscous flow motion with $v \propto f$ [8]. Ultrathin Pt/Co/Pt films with perpendicular anisotropy are systems in which one can easily study the field driven motion of quasi-1D domain walls (interfaces with elasticity due to their per-unit-length energy) in a quasi-2D Ising system with appropriate weak quenched disorder due to nanoscale inhomogeneities [1,12,16].

We have investigated domain-wall dynamics in four such films with structure Pt(4.5 nm)/Co(t_{Co})/Pt(3.5 nm)

and Co layer thickness, t_{Co} , of 0.5, 0.6, 0.7, and 0.8 nm (± 0.05 nm). The films were sputter grown at ~ 300 K on etched Si/SiO₂ substrates. Each film has a low density of efficient nucleation sites which allows us to measure domain-wall motion at high field without excessive nucleation. The films' magnetic parameters are given in Table I. First and second order effective perpendicular anisotropy fields for each sample were determined using polar magneto-optic Kerr effect (PMOKE) anisotropy measurements [18]. To estimate the wall width, Δ , we integrated these two fields into a total effective anisotropy field, H_{eff} , which includes the demagnetizing field of the perpendicularly saturated film. Out of plane PMOKE and SQUID hysteresis loops were used to determine each sample's coercive field, H_C , and saturation magnetization, M_S , respectively. The Curie temperature of each film, T_C , was deduced from the temperature dependence of the PMOKE signal at remanence. On reducing t_{Co} , both T_C and M_S are also reduced compared to their bulk values of 1388 K and 1446 erg/G cm³, respectively [19], consistent

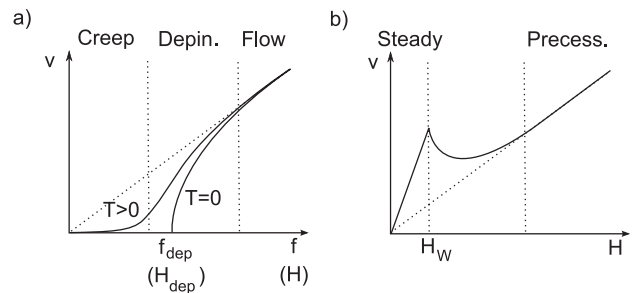


FIG. 1. (a) Theoretical variation of the velocity, v , of a 1D interface (domain wall) in a 2D weakly disordered medium submitted to a driving force, f (magnetic field, H), at zero and finite temperature, T . The creep, depinning, and flow regimes are labeled. (b) Regimes of domain-wall flow motion in an ideal ferromagnetic film without pinning. The steady and precessional linear flow regimes are separated by an intermediate regime which begins at the Walker field, H_W .

TABLE I. Co layer thickness, t_{Co} , coercive field, H_C (field sweep rate during hysteresis loop measurement ≈ 0.4 kOe/s), total integrated effective perpendicular anisotropy field, H_{eff} , and the corresponding energy, K_{eff} , Curie temperature, T_C , saturation magnetization, M_S (error $\sim 10\%$), exchange stiffness, A , zero-field domain-wall width, $\Delta = \sqrt{A/(K_{\text{eff}} + N_y 2\pi M_S^2)}$ [17], maximum possible applied field, H_{max} , limit field, H^* , for the validity of the creep velocity law [Eq. (1)], the ratio of the depinning temperature, $T_{\text{dep}} = U_C/k_B$, to the experimental temperature, $T \sim 300$ K, high field wall mobility, m (error $\sim 10\%$) and deduced values of the damping parameter, α (error $\sim 20\%$), and Walker fields, H_W (error $\sim 30\%$), for the two types of flow.

t_{Co}	H_C	H_{eff}	K_{eff}	T_C	M_S	A	Δ	H_{max}	H^*	T_{dep}/T	m	Steady		Precessional	
												α	H_W	α	H_W
nm	Oe	kOe	Merg/cm ³	K	erg/(G cm ³)	$\mu\text{erg/cm}$	nm	Oe	Oe		m/(s Oe)	Oe	Oe		
0.5	36	7.1	3.2	415	910	1.4	6.2	1080	230	9	0.028	4.0	1690	0.27	120
0.6	99	7.9	4.5	470	1130	1.6	5.5	1670	590	14	0.026	3.7	2560	0.30	210
0.7	195	5.3	3.2	520	1200	1.8	6.7	1930	750	22	0.034	3.5	2470	0.32	230
0.8	280	3.1	2.0	570	1310	2.2	8.6	1420	650	35	0.043	3.5	2460	0.31	220

with the increasing 2D character of the films and the extent of Co-Pt alloying. The exchange stiffness, A , was estimated from T_C using a model for 2D films with perpendicular anisotropy [20] and was found to be in quite good agreement with Brillouin light scattering experiments on thicker Co films [21,22].

To image the domains, we used a high resolution ($\sim 0.4 \mu\text{m}$) far-field PMOKE microscope with a cooled CCD camera. We began by saturating the sample in a field of about -3 kOe. Reverse domains were nucleated using positive high field pulses (~ 1 kOe) generated using small coils mounted close to the sample surface. The domains were then expanded under the influence of additional positive fields generated by either an electromagnet (10^0 – 10^2 Oe) or by the pulse coils which can produce field pulses up to ~ 2 kOe with well defined plateaus and variable duration [Fig. 2(a)]. The wall displacements were determined using a quasistatic technique in which an image of the domain structure was taken in zero field before

and after the application of the field pulse. The domain structure was stable in zero field during imaging. These images were then subtracted from one another [Fig. 2(b)] and the displacement measured. We recorded wall displacements for successive field pulses of the same amplitude but increasing duration (>250 ns to ensure that the pulse waveform plateau was reached). The velocity was then determined from the gradient of a linear fit to the displacement data plotted against the pulse durations. In this way, effects from the transient parts of the pulses were eliminated. Fields were applied over times ranging from ~ 250 ns to ~ 10 h, chosen such that the displacement could be reliably determined ($>10 \mu\text{m}$) and the wall remained within the field of view ($55 \mu\text{m} \times 83 \mu\text{m}$). Above H_{max} (Table I) excess nucleation prevented reliable measurement of the wall displacement.

The experimental $v(H)$ curves for the $t_{\text{Co}} = 0.5$ nm and $t_{\text{Co}} = 0.8$ nm films are shown in Fig. 2(c). Velocity-field characteristics are qualitatively consistent with predictions

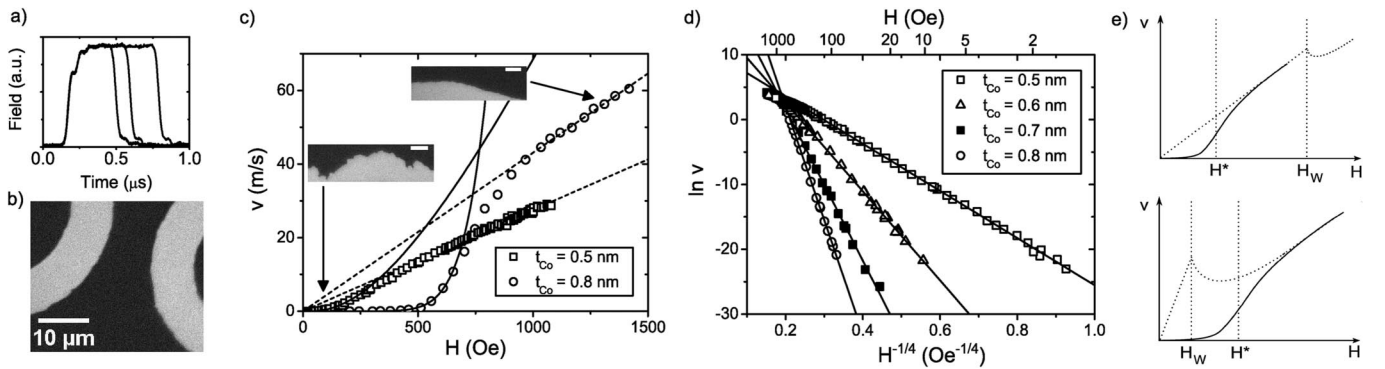


FIG. 2. (a) Waveforms of field pulses of equal magnitude but differing duration used to move the walls. (b) Subtracted domain image where the light area corresponds to the area swept out by the domain walls during a high field pulse. (c) Domain-wall velocity, v , versus applied magnetic field, H , for the $t_{\text{Co}} = 0.5$ nm and $t_{\text{Co}} = 0.8$ nm samples. We show a $v = mH$ fit to the high field flow data (dashed line) and a fit of Eq. (1) to the low field creep data (solid line). The insets show domain images in the $t_{\text{Co}} = 0.8$ nm film at fields which lie within the creep and flow regimes. The white scale bars are $5 \mu\text{m}$ long. (d) Natural logarithm of the wall velocity versus the scaled applied field to demonstrate low field creep. The solid lines are fits of the creep velocity expression [Eq. (1)]. (e) Examples of how the limited maximum applied field and low field creep prevent observation of multiple flow regimes (dotted curve) in the experimental data (solid curve—schematic only).

[Fig. 1(a)]: we evidence a low field, low velocity regime and a high field, linear regime separated by a smeared depinning region.

We begin by verifying that the low velocity regime does, in fact, correspond to creep motion for which the following velocity-field relationship is predicted ($H \ll H_{\text{dep}}$) [8]:

$$v = v_0 \exp\left[-\left(\frac{T_{\text{dep}}}{T}\right)\left(\frac{H_{\text{dep}}}{H}\right)^\mu\right]. \quad (1)$$

The depinning temperature, T_{dep} , is given by U_C/k_B , where U_C is related to the height of the disorder-induced pinning energy barrier. H_{dep} is the depinning field ($\equiv f_{\text{dep}}$), μ is a universal dynamic exponent equal to 1/4 for a 1D interface moving in a 2D weakly disordered medium [5,8], and v_0 is a numerical prefactor [8]. To verify the validity of Eq. (1) with $\mu = 1/4$ we plot $\ln v$ versus $H^{-1/4}$ in Fig. 2(d). We indeed find linear behavior at low field for all samples (corresponding to creep), proof of the universality of μ , even upon varying t_{Co} , Δ , H_{dep} , and T_{dep} (Table I).

The extent of the linear region in Fig. 2(d) is an interesting result. As can be clearly seen in Fig. 2(c), the creep law describes our data very well up to quite high fields, H^* (given in Table I), despite it being formally valid only in the small driving force limit ($H \ll H_{\text{dep}}$) [8]. H_{dep} itself is difficult to determine at finite temperature because of the thermal smearing of the depinning transition. An additional problem is that H_{dep} is related to magnetic anisotropy [1] which is itself temperature dependent. As an estimate, we set $H_{\text{dep}} = H^*$ allowing us to calculate T_{dep}/T . We find that this ratio (probed in numerical simulations [23]) increases with t_{Co} and that $T_{\text{dep}} \geq 9T$ (Table I). It has been predicted that for $T_{\text{dep}} \gg T$ an additional regime with $\ln v \propto H$ should exist in the vicinity of H_{dep} [24]. However, we see no striking evidence of this in our results. Note that such $\ln v \propto H$ behavior has been observed in ultrathin Au/Co/Au systems [25].

An additional confirmation of the validity of interface theories to describe our results comes from an analysis of the wall roughness in the creep regime. This may be quantified by examining correlations between displacements of the wall from its mean position at points separated by a distance, L : $C^2(L) = \langle [u(x) - u(x+L)]^2 \rangle \propto (L/L_C)^{2\zeta}$ [26,27]. u is the displacement of the wall from its mean position and x is the coordinate along the direction of the wall's mean orientation. L_C is a scaling length below which the interface is flat [1]. The so-called wandering exponent, ζ [1], is predicted to have a value of 2/3 for our system dimensionality [26,27]. We have verified $C^2(L) \propto L^{2\zeta}$ for the $t_{\text{Co}} = 0.6$ nm and $t_{\text{Co}} = 0.8$ nm films and have found values for ζ of 0.7 ± 0.1 and 0.66 ± 0.06 , respectively, in agreement with theory [26,27] and previous experimental results [1]. In the creep regime the walls in the 0.5 nm film are smoother than those in the 0.8 nm film, testament to the 0.5 nm film's lower T_{dep} and H^* .

In the high field regime, outside that of creep, walls in all of the films become significantly smoother [insets of Fig. 2(c)], indicative of the reduced relevance of the disorder. We find that the velocity in this high field regime can be fitted well using $v = mH$, with m the wall mobility, consistent with predictions from moving interface theories. This is the first direct experimental measurement of interface flow in a weakly disordered system [28].

Rather than disorder, dissipation limits the wall velocity in the flow regime. Here, dissipation is characterized by the magnetic damping parameter, α , which is related to the wall mobility, m [13–15]. In contrast to the standard elastic interface problem, in magnetic systems two separate regimes of linear flow are expected (each with $v = mH$ but different mobilities) [Fig. 1(b)]. This is due to a change in the internal dynamics of the wall above a critical field known as the Walker field, H_W [13–15]. Below H_W the domain-wall motion is steady with the mobility given by $m = \gamma\Delta/\alpha$, where γ is the gyromagnetic ratio [1.76×10^7 (Oe s) $^{-1}$]. Sufficiently above H_W there exists a second linear flow regime in which the magnetization within the domain wall precesses. The mobility in this precessional flow regime is lower than that of the steady one: $\langle m \rangle = \gamma\Delta/(\alpha + \alpha^{-1})$. These two linear flow regimes, together with a nonlinear intermediate regime [13], have been recently observed in NiFe nanowires in which pinning is minimal [29,30]. The Walker field can be written as $H_W = N_y 2\pi\alpha M_S$ [17,31], where N_y is the demagnetizing factor across the wall, given as $t_{\text{Co}}/(t_{\text{Co}} + \Delta)$ in a simple approximation [17].

The observation of only one linear regime in Fig. 2(c) can be explained by two scenarios. First, H_W could be beyond H_{max} , meaning that the flow that we observe is steady flow [upper part of Fig. 2(e)]. From the steady flow mobility expression, we can then calculate α , which we find to be about 4 for each film. The corresponding H_W values are consistent with the steady flow assumption, being above H_{max} . The other possibility is that H_W is below H^* , in which case we would see only precessional flow since the steady flow would be obscured by the creep regime [lower part of Fig. 2(e)]. The precessional flow mobility expression yields α values on the order of 0.3, resulting in H_W values which are indeed below H^* . All values are given in Table I.

On the basis of the relative magnitudes of the α values for each type of flow motion, we are inclined to accept those corresponding to precessional motion. Although quite large, these α values are, in fact, on the same order of magnitude as those found via other techniques in ultrathin Pt/Co/Pt multilayers [32,33] and thicker Cr-Pt-Co systems [34,35]. Very broad linewidths in ferromagnetic resonance (FMR) measurements prevented a reliable independent determination of α for the samples studied here. However, FMR measurements on slightly thicker Pt/Co/Pt films (with in-plane anisotropy) yielded α values on the order of those in Table I (e.g., 0.22 for $t_{\text{Co}} = 1.4$ nm).

Considering the significant error in α and the limited range of t_{Co} (due to a magnetic reorientation transition at ~ 0.9 nm), we cannot comment seriously on the dependence of α on t_{Co} in Table I. We also note contributions from less easily quantified errors in our determination of A , N_y , and Δ . Reduction of H_{dep} could allow for direct observation of the change in dynamics at H_W which would confirm our analysis and provide results complementary to recent measurements on in-plane magnetized nanowires [29,30]. Note that our wall mobilities are smaller than those measured in NiFe nanowires [29,30] and films [36] which may be attributed to the narrower walls and higher damping in our films.

In conclusion, we have experimentally obtained for the first time the complete velocity-field characteristics of a 1D interface in a 2D weakly disordered medium through direct measurements of domain-wall motion in ultrathin Pt/Co/Pt films. This has allowed us to examine both pinning and dissipation processes as well as test the validity of general theories concerning interface dynamics. We also observed changes in the wall profile on moving from one motion regime to another. Finally, we determined a value for the magnetic damping parameter, α , which describes the dissipation occurring during flow motion.

P. J. M. acknowledges support from the Australian government and a Marie Curie Action (No. MEST-CT-2004-514307). P. J. M., A. M., J. F., and R. L. S. were supported by the FAST program (French-Australian Science and Technology). P. J. M. and R. L. S. acknowledge the Australian Research Council. This work was partly done in the frame of the ACI contract, PARCOUR. We thank H. Hurdequint for FMR measurements, R. C. Woodward for assistance with SQUID measurements, S. Wiebel for assistance with initial experiments, and J. P. Adam for useful discussions.

*metaxas@lps.u-psud.fr

- [1] S. Lemerle, J. Ferré, C. Chappert, V. Mathet, T. Giamarchi, and P. Le Doussal, *Phys. Rev. Lett.* **80**, 849 (1998).
- [2] L. Krusin-Elbaum, T. Shibauchi, B. Argyle, L. Gignac, and D. Weller, *Nature (London)* **410**, 444 (2001).
- [3] V. Repain, M. Bauer, J. P. Jamet, J. Ferré, A. Mougin, C. Chappert, and H. Bernas, *Europhys. Lett.* **68**, 460 (2004).
- [4] P. Paruch, T. Giamarchi, T. Tybell, and J. M. Triscone, *J. Appl. Phys.* **100**, 051608 (2006).
- [5] G. Blatter, M. V. Feigel'man, V. B. Geshkenbien, A. I. Larkin, and V. M. Vinokur, *Rev. Mod. Phys.* **66**, 1125 (1994).
- [6] H. Fukuyama and P. A. Lee, *Phys. Rev. B* **17**, 535 (1978).
- [7] P. G. de Gennes, *Rev. Mod. Phys.* **57**, 827 (1985).
- [8] P. Chauve, T. Giamarchi, and P. Le Doussal, *Phys. Rev. B* **62**, 6241 (2000).
- [9] T. Nattermann, V. Pokrovsky, and V. M. Vinokur, *Phys. Rev. Lett.* **87**, 197005 (2001).
- [10] S. Brazovskii and T. Nattermann, *Adv. Phys.* **53**, 177 (2004).
- [11] X. Chen, O. Sichelshmidt, W. Kleemann, O. Petravic, C. Binek, J. B. Sousa, S. Cardoso, and P. P. Freitas, *Phys. Rev. Lett.* **89**, 137203 (2002).
- [12] W. Kleemann, J. Rhensius, O. Petravic, J. Ferré, J. P. Jamet, and H. Bernas, *Phys. Rev. Lett.* **99**, 097203 (2007).
- [13] J. C. Slonczewski, *Int. J. Magn.* **2**, 85 (1972).
- [14] N. L. Schryer and L. R. Walker, *J. Appl. Phys.* **45**, 5406 (1974).
- [15] A. P. Malozemoff and J. C. Slonczewski, *Magnetic Domain Walls in Bubble Materials* (Academic Press, New York, 1979).
- [16] J. Ferré, in *Spin Dynamics in Confined Magnetic Structures I*, edited by B. Hillebrands and K. Ounadjela (Springer-Verlag, Berlin, Heidelberg, 2002), Vol. 83, pp. 127–168.
- [17] A. Mougin, M. Cormier, J. P. Adam, P. J. Metaxas, and J. Ferré, *Europhys. Lett.* **78**, 57007 (2007).
- [18] V. Grolier, J. Ferré, A. Maziewski, E. Stefanowicz, and D. Renard, *J. Appl. Phys.* **73**, 5939 (1993).
- [19] M. Mansuripur, *The Physical Principles of Magneto-Optical Recording* (Cambridge University Press, Cambridge, U.K., 1995).
- [20] P. Bruno, *Mater. Res. Soc. Symp. Proc.* **231**, 299 (1992).
- [21] X. Liu, M. M. Steiner, R. Sooryakumar, G. A. Prinz, R. F. C. Farrow, and G. Harp, *Phys. Rev. B* **53**, 12166 (1996).
- [22] M. Grimsditch, E. E. Fullerton, and R. L. Stamps, *Phys. Rev. B* **56**, 2617 (1997).
- [23] A. B. Koltun, A. Rosso, and T. Giamarchi, *Phys. Rev. Lett.* **94**, 047002 (2005).
- [24] M. Müller, D. A. Gorokhov, and G. Blatter, *Phys. Rev. B* **63**, 184305 (2001).
- [25] A. Kirilyuk, J. Ferré, V. Grolier, J. P. Jamet, and D. Renard, *J. Magn. Magn. Mater.* **171**, 45 (1997).
- [26] D. A. Huse and C. L. Henley, *Phys. Rev. Lett.* **54**, 2708 (1985).
- [27] D. A. Huse, C. L. Henley, and D. S. Fisher, *Phys. Rev. Lett.* **55**, 2924 (1985).
- [28] Our flow regime corresponds to “slide” evidenced from ac susceptibility measurements in [12].
- [29] G. S. D. Beach, C. Nistor, C. Knutson, M. Tsoi, and J. L. Erskine, *Nature Mater.* **4**, 741 (2005).
- [30] M. Hayashi, L. Thomas, C. Rettner, R. Moriya, and S. S. P. Parkin, *Nature Phys.* **3**, 21 (2007).
- [31] D. G. Porter and M. J. Donahue, *J. Appl. Phys.* **95**, 6729 (2004).
- [32] C. H. Back and H. C. Siegmans, *J. Magn. Magn. Mater.* **200**, 774 (1999).
- [33] A. Barman, S. Wang, O. Hellwig, A. Berger, E. E. Fullerton, and H. Schmidt, *J. Appl. Phys.* **101**, 09D102 (2007).
- [34] C. H. Back, R. Allenspach, W. Weber, S. S. P. Parkin, D. Weller, E. L. Garwin, and H. C. Siegmans, *Science* **285**, 864 (1999).
- [35] I. Tudosa, C. Stamm, A. B. Kashuba, F. King, H. C. Siegmans, J. Stohr, G. Ju, B. Lu, and D. Weller, *Nature (London)* **428**, 831 (2004).
- [36] K. Fukumoto, W. Kuch, J. Vogel, J. Camarero, S. Pizzini, F. Offi, Y. Pennec, M. Bonfim, A. Fontaine, and J. Kirschner, *J. Magn. Magn. Mater.* **293**, 863 (2005).